ORIGINAL ARTICLE

*Journal of Cachexia, Sarcopenia and Muscle* 2019; **10**: 574–585
Published online 15 March 2019 in Wiley Online Library (wileyonlinelibrary.com) **DOI:** 10.1002/jcsm.12415

# Muscle fat quantification using magnetic resonance imaging: case–control study of Charcot–Marie–Tooth disease patients and volunteers

Hyun Su Kim[1], Young Cheol Yoon[1]*, Byung-Ok Choi[2], Wook Jin[3] & Jang Gyu Cha[4]

[1]*Department of Radiology, Samsung Medical Center, School of Medicine, Sungkyunkwan University, Seoul, South Korea,* [2]*Department of Neurology, Samsung Medical Center, School of Medicine, Sungkyunkwan University, Seoul, South Korea,* [3]*Department of Radiology, Kyung Hee University Hospital at Gangdong, Seoul, South Korea,* [4]*Department of Radiology, Soonchunhyang University Bucheon Hospital, Bucheon, South Korea*

## Abstract

**Background** This study aimed to evaluate the potential value of 3D multiple gradient echo Dixon-based magnetic resonance imaging (MRI) sequence as a tool for thigh intramuscular fat quantification in Charcot–Marie–Tooth disease (CMT) patients.
**Methods** A prospective comparison study comprising 18 CMT patients and 18 age/sex-matched volunteers was performed. MRI including 3D multiple gradient echo Dixon-based imaging was performed for each subject. Region of interest analyses were performed at the upper and lower third of both thighs. The two-sample *t*-test or Wilcoxon rank sum test was used for intergroup comparison of the mean muscle fat fraction. Intraclass correlation coefficients were used to evaluate the inter-observer agreement and test–retest reproducibility. Semiquantitive analysis using the Goutallier classification (Grades 0–4) was performed on T1-weighted images in upper thigh muscles. For Goutallier Grade 0 muscles, comparison of the mean intramuscular fat fraction between volunteers and CMT patients was performed.
**Results** The interobserver agreements were excellent for all measurements (intraclass correlation coefficients $> 0.8$). Mean muscle fat fractions were significantly higher in all the measured muscles of CMT patients ($P < 0.05$) except in the adductor magnus in the upper thigh ($P = 0.109$). Goutallier Grade 0 muscles of the CMT patients showed a significantly higher mean fat fraction compared with that of the volunteers ($P < 0.05$).
**Conclusions** 3D multiple gradient echo Dixon-based MRI is a reproducible and sensitive technique which can reveal a significant difference in the fat fraction of thigh muscle, including comparison between Goutallier Grade 0 muscles, between CMT patients and volunteers.

**Keywords** Magnetic resonance imaging; Multiple gradient echo Dixon; Muscle fat quantification; Charcot–Marie–Tooth disease

*Received: 28 August 2018; Accepted: 27 January 2019*
**Correspondence to: Young Cheol Yoon, Department of Radiology, Samsung Medical Center, School of Medicine, Sungkyunkwan University, 81 Ilwon-Ro, Gangnam-gu, Seoul 135-710, South Korea. Email: youngcheol.yoon@gmail.com*

## Introduction

Charcot–Marie–Tooth disease (CMT) represents a group of hereditary neuromuscular disorders linked to various gene mutations responsible for either primary axonal degeneration or primary myelin changes with eventual axonal degeneration.[1] The consequence is peripheral neuropathy with a characteristic distal predominant limb-muscle wasting and sensory loss.[1] It has been reported that there is a substantial variability in the clinical course of the disease among various subtypes and even within the same subtype of the disease.[1,2] Thus, careful monitoring of patients is necessary. Currently, there exists no approved pharmacological treatment and supportive measures remain the main treatment for CMT, but several preclinical and clinical studies using pharmacological agents have shown promising results.[3–6] In addition, recent

advances in knowledge regarding the genetic basis of CMT with numerous genes identified to be associated with CMT suggest potentials for developing possible treatment options for the disease in the future.[7] In this regard, an objective and reliable tool for assessing the status of patients including the evaluation of treatment response would be necessary.

In the management of CMT patients, careful assessment and monitoring of the affected muscle is important. One of the common problems encountered in these patients in clinical practice is the lack of a standardized method to assess muscle degeneration. Numerous scoring systems, which composed of multiple clinical parameters including limb strength, have been developed for diagnosis and monitoring of CMT patients.[8–10] Despite several revisions, there remain some limitations including issues regarding inter-rater and intra-rater agreement.[8] Muscle biopsy may provide some information on muscle fat infiltration, but it is impractical to use it on a regular basis due to its invasiveness and limited number of biopsy sites, which does not represent the true state of the disease with multiple muscles involved.

Magnetic resonance imaging (MRI) allows general visual assessment for the degree and distribution of intramuscular fat infiltration in multiple muscle compartments, which is a commonly associated finding in CMT patients.[11,12] A semi-quantitative grading system using a conventional T1-weighted imaging sequence described by Goutallier *et al*. is widely used scoring system for various muscular abnormalities.[13] This system has a significant shortcoming of being highly observer dependent[14,15] and lacking quantitative data. Furthermore, because this classification relies on macroscopic fat signal and only has five grades, it is not optimized for assessment of early fat infiltration or interval progression that is not severe enough to result in change of grades.[16] Dixon MRI is an emerging imaging technique for fat fraction measurement that exploits the capability to differentiate the individual contributions of water and fat in each voxel of tissue using the chemical shift difference between the two.[17] Recent Dixon-based MRI techniques generate fat fraction maps that allows direct quantitative measurement of the fat proportion within the designated region of interest (ROI).[18] Studies have reported encouraging results with using Dixon-based techniques for fat quantification in skeletal muscle.[15,16] Given the significant clinical implication of the muscle assessment in CMT patient management, a reproducible quantitative imaging parameter acquired through Dixon-based MRI would be desirable.

In our study, the potential value of intramuscular fat quantification using a 3D multiple gradient echo Dixon-based MRI sequence was sought by performing a prospective comparison study encompassing CMT patients and volunteers. We performed analyses in thigh, where fat infiltration is less prominent compared to that in calf due to the predominant nature of distal muscle involvement in CMT. Furthermore, we aimed to evaluate the potential of 3D multiple gradient echo Dixon sequence in terms of sensitivity by comparing the fat fraction of grossly normal muscle, based on Goutallier grading, between CMT patients and volunteers.

## Materials and methods

### *Study population*

The study was approved by our institutional review board. Between February and June 2017, 18 patients diagnosed with CMT Type I by genetic analysis and electrophysiologic study prospectively underwent MRI. Seventeen patients who received genetic analysis were diagnosed as CMT Type IA. One patient who did not receive genetic testing was diagnosed with CMT Type I based on electrophysiologic study and clinical history. The cohort was confined to patients aged between 20 and 40 years old (mean ± standard deviation: 30.1 ± 4.3 years; range: 23–37 years; 8 male and 10 female participants). Patients had no contraindication for MRI, such as claustrophobia or metallic implant. A public notice was posted to recruit 18 age-matched and sex-matched volunteers with no history of peripheral neuropathy or other pathologic condition in the lower extremities.

A neurologist (B.C, with 21 years of experience) performed a neurologic examination to assess for signs of abnormality prior to MRI. Finally, 18 age/sex-matched healthy volunteers (mean age: 28.2 ± 1.2 years; age range: 20–36 years; 8 male and 10 female participants) were recruited. All participants gave written informed consent prior to MRI. No participant dropped out, so data acquired from 18 subjects in each group were used for analyses.

### *Magnetic resonance imaging acquisition*

Magnetic resonance imaging (MRI) was obtained using a 3.0-T MRI system (Ingenia; Philips Healthcare, Best, the Netherlands) with a 16-channel anterior coil and posterior built-in coil. The following MRI sequences were obtained for morphologic imaging: coronal and axial T1-weighted turbo spin echo sequences, and axial T2-weighted Dixon sequence. From the Dixon sequence, water-only, fat-only, in-phase, and out-of-phase images were produced. The MRI protocols are detailed in Table 1.

A 3D multiple gradient echo Dixon-based MRI sequence (mDixon-Quant; Philips Healthcare, Best, the Netherlands) was obtained for fat fraction quantification which sampled six-echo data. Images were obtained for the pelvic girdle and the thighs at levels from the anterior inferior iliac spine through the distal end of the femur, in the axial plane. Fat and water-only images were consequentially reconstructed, thereby automatically generating axial fat fraction maps with correction for confounding effects of T2* decay.

**Table 1.** Summary of magnetic resonance imaging parameters

| Imaging parameters | T1-weighted TSE imaging in axial plane | T1-weighted TSE imaging in coronal plane | T2-weighted Dixon imaging in axial plane | mDixon-Quant |
|---|---|---|---|---|
| Repetition time (ms) | 613.7 | 450–650 | 4635.5 | 6.6 |
| Echo time (ms) | 16.7 | 15 | 80 | 1.01, 1.91, 2.81, 3.71, 4.61, 5.51 |
| Flip angle (°) | 90 | 90 | 90 | 3 |
| No. of signals averaged | 1 | 1 | 1 | 2 |
| Reconstructed voxel size (mm) | 0.68 | 0.68 | 0.68 | 1.82 |
| Matrix size | 320 × 320 | 320 × 317 | 320 × 320 | 192 × 192 |
| Field of view (mm) | 350 × 350 | 350 × 350 | 350 × 350 | 350 × 350 |
| Section thickness (mm) | 2 | 5 | 2 | 6 |
| Gap (mm) | 1 | 0.5 | 1 | 0 |
| Number of slices | 67 | 25 | 67 | 140 |
| Imaging time (s) | 162 | 200 | 194 | 72.5 |

mDixon-Quant, 3D multiple gradient echo Dixon-based sequence for fat quantification; N/A, not applicable; TSE, turbo-spin echo.

## *Data analysis*

Water-only images and fat fraction maps were loaded into image-processing software (IntelliSpace Portal, version 5.0; Philips Healthcare). The segmentation of all muscle compartments was manually performed by two independent radiologists (Y.C.Y and H.S.K, with 14 and 5 years of experience in musculoskeletal radiology, respectively) who were blinded to the clinical information. ROIs were initially drawn on water-only images because it offers better visualization of muscle boundaries. Using copy-and-paste function at the workstation, ROIs with identical shape, size, and position were generated on fat fraction maps.

Thigh muscles were segmented to define seven muscles: rectus femoris, vastus lateralis, vastus medialis, biceps femoris (long head), semitendinosus, adductor magnus, and gracilis (Figures 1–3). These muscles were chosen for analysis as they were constantly visualized with relatively discrete margins. Two levels were considered to measure muscle fat fraction—the upper and lower third of both thighs. Among axial image slices containing the uppermost part of the femoral heads to the lower most part of the femoral condyles, these two levels were determined using the slice number of the axial images. Measurement was not performed for the biceps femoris in the upper third and adductor magnus in the lower third due to the small cross-sectional area and inconsistent demonstration of muscle. The manual drawing of ROI was performed so that the boundaries were within 1–2 mm from the muscle fascia. A training session was conducted prior to the measurements, to familiarize both radiologists with the areas of measurement and defining ROI for muscle. One radiologist again drew ROIs that best fit the muscle boundaries to measure the cross-sectional area of the muscles at the upper and lower third of both thighs.

All subjects were examined two times to evaluate the test–retest reproducibility of the 3D multiple gradient echo Dixon-based MRI. Using copy-and-paste function, each radiologist independently generated ROIs on fat fraction maps of the second image set.

## *Semiquantitative assessment*

Two radiologists analysed T1-weighted images of thigh muscles and graded the presence of fatty infiltration independently based on a five-point semiquantitative scale described by Goutallier *et al.*[19]: Grade 0, normal; Grade 1, some fatty streaks; Grade 2, less fat than muscle; Grade 3, fatty degeneration of 50%; Grade 4, fatty infiltration of more than 50%. Radiologists were blinded to the clinical information, and analyses were performed at the same level where the fat fraction measurement for the upper thigh muscle was performed on the fat fraction map.

## *Clinical assessment*

Demographic and clinical data of the CMT patients are shown in Table 2. Disease duration was determined by asking the patients when their symptoms, such as distal muscle weakness, foot deformity, and/or sensory change, first appeared. The severity of CMT was evaluated using the functional disability scale[20] and the CMT neuropathy score (CMTNS).[21] The British Medical Research Council scale was used to assess the thigh muscle strength.[22] Knee extension and flexion were tested on both sides. One CMT patient showed Medical Research Council Grade 4+ for knee extension for both sides while all the other patients showed no abnormality. None of the patients experienced subjective weakness regarding thigh movements. Electrophysiologic study result in the peroneal and tibial nerves of the CMT patients are shown in Table 3.

## *Statistical analysis*

Statistical analyses were performed using SAS version 9.4 (SAS Institute, Cary, NC, USA). Interobserver agreements and test–retest reproducibility of muscle fat quantification were calculated using intraclass correlation coefficients, interpreted as follows: 0.81–1.00, *excellent*; 0.61–0.80, *good*, and ≤0.60, *poor*

**Figure 1** An example of semiquantitative analysis and region of interest (ROI) measurement performed for intramuscular fat quantification in upper thighs of a 33 year-old male volunteer. All the muscles of upper thigh were Graded 0 on axial T1-weighted image (A) based on semiquantitative scale described by Goutallier *et al*. ROIs were initially drawn in muscles of corresponding level on water-only image (B) acquired from 3D multiple gradient echo Dixon-based magnetic resonance imaging. Using copy-and-paste function, ROIs with identical shape, size, and position were generated on fat fraction map (C). Measured intramuscular fat fraction ranged from 1.33 to 7.36%. [Rectus femoris, 1.48% (left) and 2.48% (right); vastus lateralis, 2.35% and 3.04%; vastus medialis, 1.33% and 1.68%; semitendinosus, 2.85% and 4.52%; adductor magnus, 2.92% and 2.50%; gracilis, 6.94% and 7.36%]. Notes: AM, adductor magnus; G, gracilis; RF, rectus femoris; S, semitendinosus; VL, vastus lateralis; VM, vastus medialis.

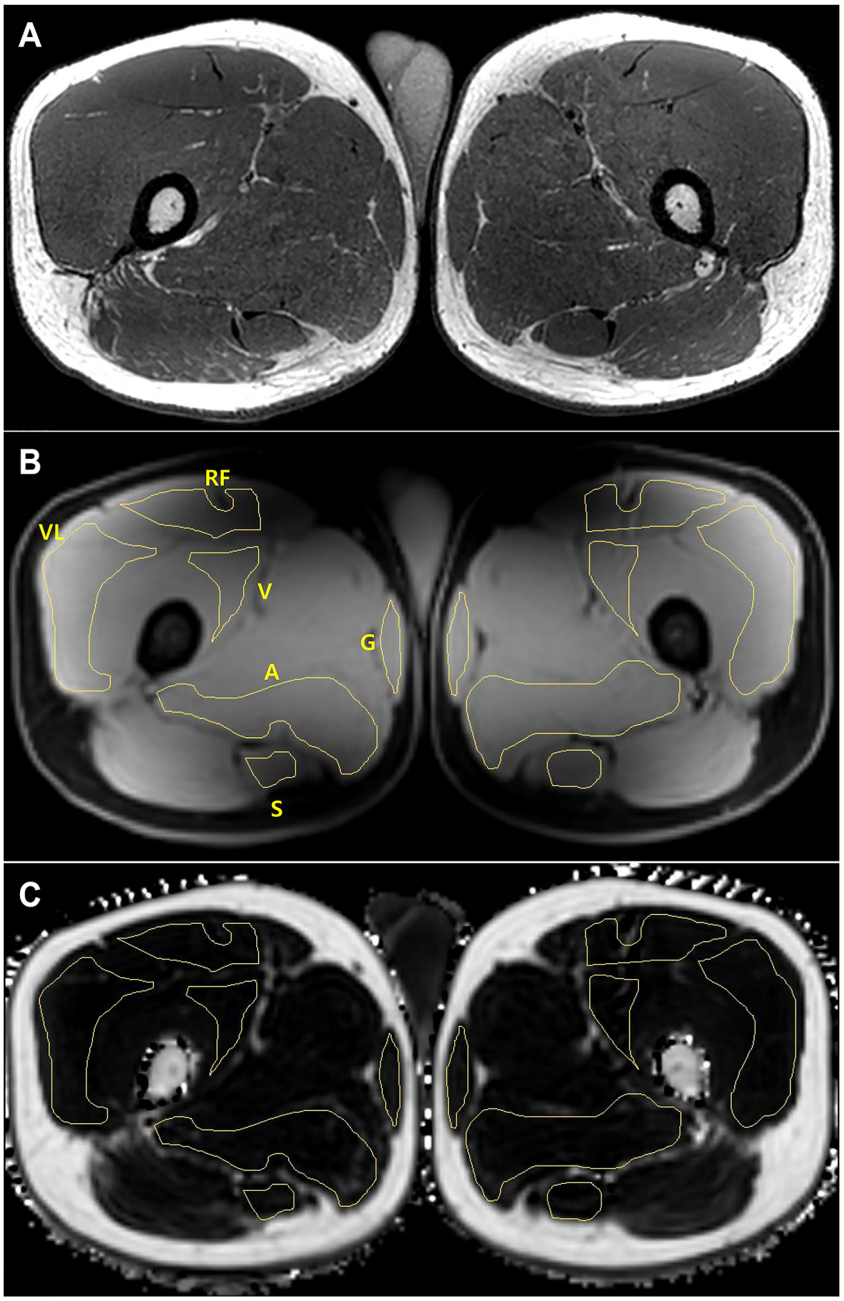


*agreement*. Interobserver agreement of semiquantitative assessment was performed using Cohen's kappa analysis, interpreted as follows: 0.81–1.00, *almost perfect*; 0.61–0.80, *substantial*; 0.41–0.60, *moderate*; 0.21–0.40, *fair*; and ≤0.20, *slight* agreement. Using Bland–Altman analysis, mean difference and standard deviation of interobserver agreements and test–retest reproducibility were also acquired.

Comparison of mean muscle fat fraction and cross-sectional area in both thighs between CMT patients and volunteers was conducted using the Wilcoxon rank sum test. For

**Figure 2** An example of region of interest (ROI) measurement performed for intramuscular fat quantification in lower thighs of 35 year-old male Charcot–Marie–Tooth disease patient. ROIs were initially drawn on water-only image (A) acquired from 3D multiple gradient echo Dixon-based magnetic resonance imaging. ROIs with identical shape, size, and position were generated on fat fraction map (B). Measured intramuscular fat fraction ranged from 2.87% to 20.79%. [Rectus femoris, 7.03% (left) and 2.87% (right); vastus lateralis, 7.37% and 7.35%; vastus medialis, 5.78% and 4.72%; biceps femoris, 20.79% and 17.30%; semitendinosus,13.28% and 8.74%; gracilis, 16.18% and 10.36%]. Notes: BF, biceps femoris; G, gracilis; RF, rectus femoris; S, semitendinosus; VL, vastus lateralis; VM, vastus medialis.

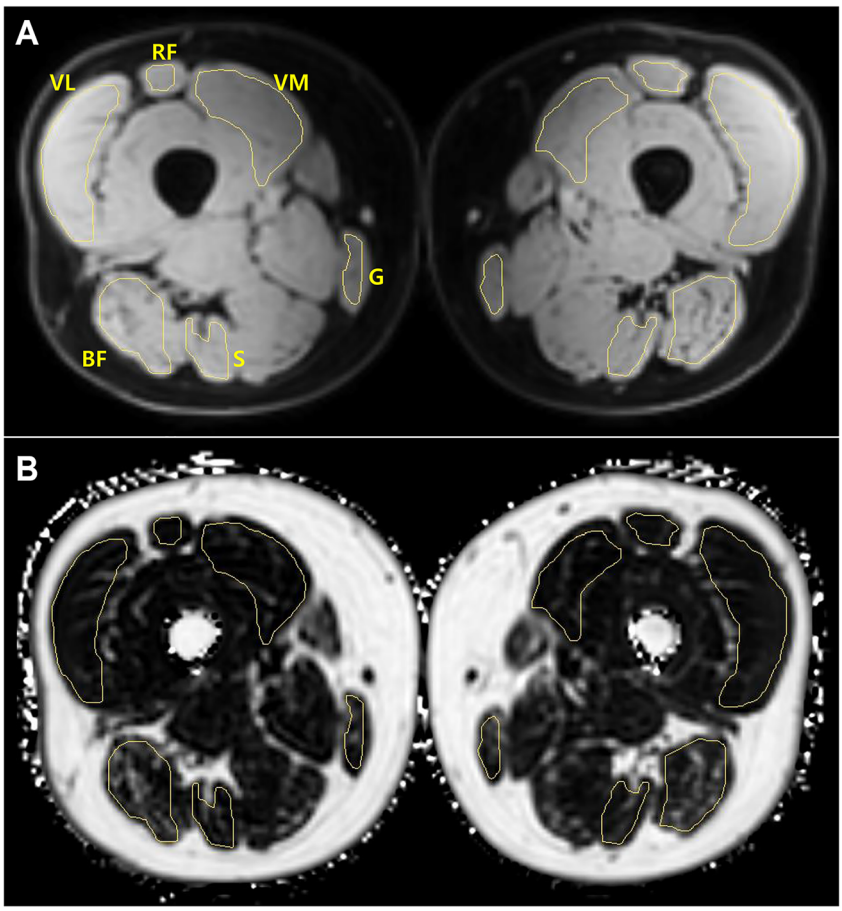


thigh muscles classified as Goutallier Grade 0, comparison of mean intramuscular fat fraction between the two groups were performed using the Wilcoxon rank sum test. Fat fraction of the upper and lower thigh muscles (rectus femoris, vastus lateralis, vastus medialis, and semitendinosus) was compared using Wilcoxon signed rank test in CMT patients.

The relationship between the thigh muscle fat fraction and clinical data (i.e. disease duration, CMTNS, and functional disability scale) were evaluated using Spearman's correlation analysis in the CMT patients. Comparison of body mass index (BMI) between both groups was conducted using the Wilcoxon rank sum test to confirm the presence of a significant difference that may affect the intramuscular fat fraction. In addition, Spearman's correlation analysis was performed to find possible correlation between BMI and thigh muscle fat fraction in both groups.

## Result

Both sets of 3D multiple gradient echo Dixon-based MRI obtained from one volunteer and one CMT patient, respectively, showed fat-water swap. Also, a single set of 3D multiple gradient echo Dixon-based MRI in one volunteer showed fat-water swap. These image sets were not included in the analysis. Thus, interobserver agreement evaluation and comparison of muscle fat fraction between the two groups were conducted for 17 volunteers and 17 CMT patients. Semiquantitative analyses of the upper thigh muscles were performed in the same study population. Test–retest reproducibility evaluation was performed for 33 subjects, which composed of 16 volunteers and 17 CMT patients. There was no significant difference in BMI between the two groups ($P$ = 0.270; volunteers: median ± standard deviation, 21.60 ± 3.09;

**Figure 3** An example of semiquantitative analysis and region of interest (ROI) measurement performed for intramuscular fat quantification in upper thighs of a 36 year-old male Charcot–Marie–Tooth disease patient. All the muscles of upper thigh were Graded 0 on axial T1-weighted image (A) based on semiquantitative scale described by Goutallier *et al*. ROIs were initially drawn in muscles of corresponding level on water-only image (B) acquired from 3D multiple gradient echo Dixon-based MRI. Using copy-and-paste function, ROIs with identical shape, size, and position were generated on fat fraction map (C). Measured intramuscular fat fraction ranged from 3.54% to 7.29%. [Rectus femoris, 4.71% (left) and 4.64% (right); vastus lateralis, 6.86% and 4.49%; vastus medialis, 4.33% and 5.04%; semitendinosus, 4.47% and 6.33%; adductor magnus, 3.54% and 3.92%; gracilis, 7.29% and 7.00%]. Notes: AM, adductor magnus; G, gracilis; RF, rectus femoris; S, semitendinosus; VL, vastus lateralis; VM, vastus medialis.

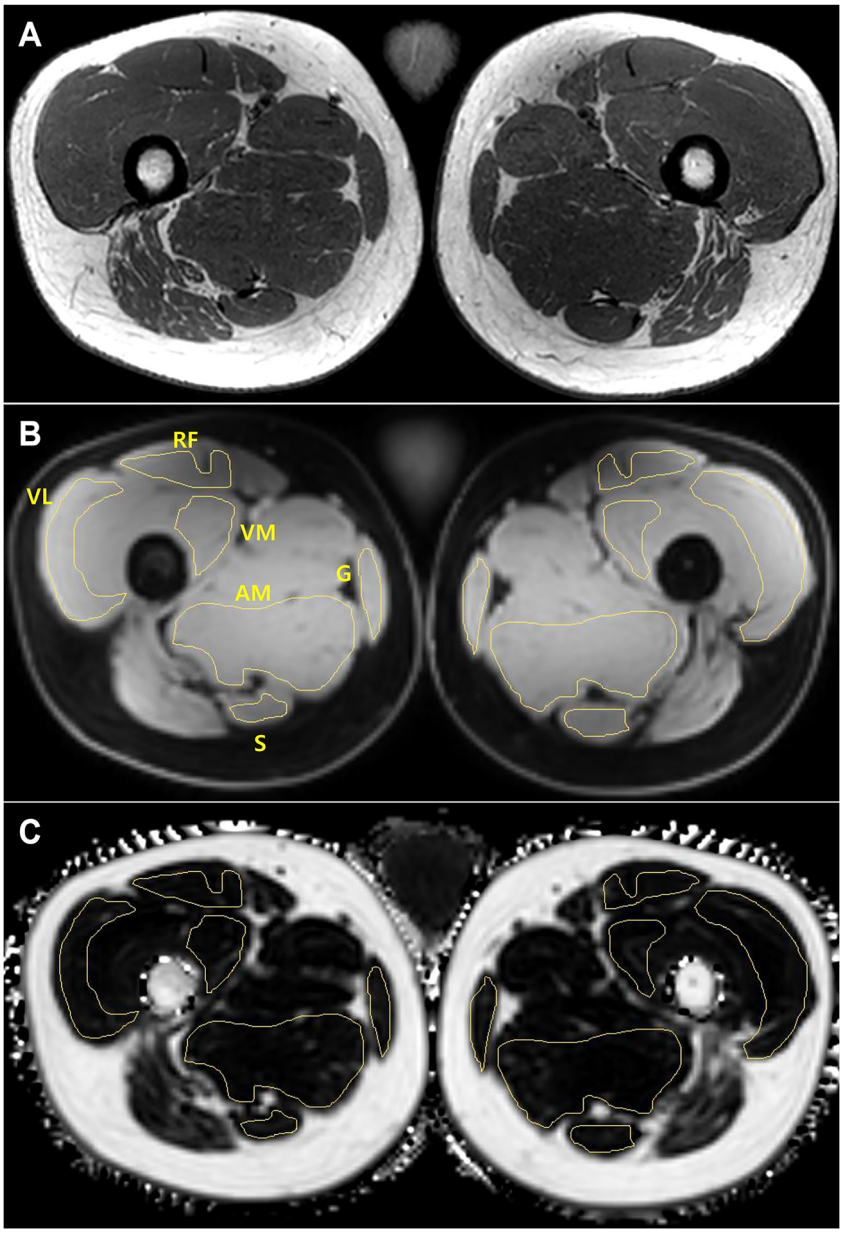


interquartile range, 20.60–25.10; CMT patients: median ± standard deviation, 23.06 ± 4.99; interquartile range, 21.48–27.63).

The interobserver agreements in the muscle fat fraction measurement were excellent for all fat quantification analyses (Table 4). The result of the test–retest reproducibility of quantitative fat fraction measurement was excellent in both reviewers' evaluation except for the adductor magnus muscle in the left upper thigh measured by Reviewer 1, which showed good agreement (intraclass correlation coefficients = 0.67). Data obtained by Reviewer 1 using the first image set were used for comparison of the intramuscular fat

**Table 2.** Demographic and clinical data of the Charcot–Marie–Tooth disease patients

| Patient number | Gender | Age | Disease duration (years) | Charcot–Marie–Tooth neuropathy score | Functional disability scale | Knee extension[a] (left/right) | Knee flexion[a] (left/right) |
|---|---|---|---|---|---|---|---|
| 1 | Male | 22 | 11 | 5 | 1 | 5/5 | 5/5 |
| 2 | | 24 | 2 | 7 | 1 | 5/5 | 5/5 |
| 3 | | 26 | 0 | 14 | 2 | 5/5 | 5/5 |
| 4 | | 27 | 12 | 16 | 2 | 5/5 | 5/5 |
| 5 | | 29 | 16 | 16 | 2 | 5/5 | 5/5 |
| 6 | | 34 | 19 | 11 | 1 | 5/5 | 5/5 |
| 7 | | 36 | 29 | 21 | 3 | 5/5 | 5/5 |
| 8 | Female | 20 | 5 | 15 | 3 | 5/5 | 5/5 |
| 9 | | 22 | 6 | 9 | 1 | 5/5 | 5/5 |
| 10 | | 23 | 2 | 7 | 1 | 5/5 | 5/5 |
| 11 | | 28 | 11 | 18 | 2 | 5/5 | 5/5 |
| 12 | | 32 | 30 | 9 | 1 | 5/5 | 5/5 |
| 13 | | 35 | 16 | 16 | 2 | 5/5 | 5/5 |
| 14 | | 33 | 33 | 6 | 1 | 5/5 | 5/5 |
| 15 | | 25 | 12 | 17 | 2 | 4+/4+ | 5/5 |
| 16 | | 34 | 5 | 6 | 1 | 5/5 | 5/5 |
| 17 | | 31 | 18 | 9 | 1 | 5/5 | 5/5 |

[a]Assessment based on British Medical Research Council scale.

**Table 3.** Electrophysiologic study result of the Charcot–Marie–Tooth disease patients

| | Peroneal nerve | | | Tibial nerve | | |
|---|---|---|---|---|---|---|
| Patient number | TL (ms) (left/right) | CMAP (mV) (left/right) | NCV (m/s) (left/right) | TL (ms) (left/right) | CMAP (mV) (left/right) | NCV (m/s) (left/right) |
| 1 | 16.3/16.8 | 0.9/2.6 | 16.5/16.9 | 14.5/12.3 | 3.2/4.7 | 17.4/17.4 |
| 2 | 13.5/13.2 | 0.4/1.2 | 18.7/18.2 | 10.0/10.2 | 7.8/8.0 | 20.8/19.1 |
| 3 | 12.3/12.5 | 1.5/0.6 | 16.3/19.0 | 8.5/8.2 | 0.5/0.3 | 14.4/15.2 |
| 4 | A/A | A/A | A/A | 10.6/11.4 | 1.0/0.5 | 14.4/12.7 |
| 5 | 11/A | 1.6/A | 13.0/A | 12.0/12.2 | 0.2/0.6 | 16.2/14.3 |
| 6 | 9/7.4 | 2.7/2.7 | 20.8/20.2 | 11.9/8.6 | 0.7/3.3 | 20.8/23.4 |
| 7 | 9.4/10.2 | 0.8/0.6 | 17.6/16.4 | 7.8/7.1 | 2.3/2.0 | 18.6/16.4 |
| 8 | A/16.5 | A/0.3 | A/13.7 | 20.1/21.2 | 0.3/0.9 | 17.3/15.1 |
| 9 | 9.1/9.0 | 1.1/1.8 | 24.9/21.8 | 9.9/7.5 | 4.9/6.3 | 28.4/26.5 |
| 10 | 11.6/11.1 | 0.8/0.8 | 15.3/15.1 | 10.2/10.7 | 3.6/4.1 | 17.1/18.5 |
| 11 | A/A | A/A | A/A | 11.3/16.9 | 0.2/0.4 | A/19.2 |
| 12 | 7.6/8.2 | 4.2/3.1 | 34.2/31.8 | 5.0/9.1 | 10.0/3.3 | 26.7/36.6 |
| 13 | A/A | A/A | A/A | A/A | A/A | A/A |
| 14 | 12.9/9.6 | 2.9/4.6 | 17.2/19.5 | 10.5/10.5 | 7.7/7.7 | 19.3/19.3 |
| 15 | A/A | A/A | A/A | 10.4/12.6 | 0.6/0.5 | 13.7/10.0 |
| 16 | A/A | A/A | A/A | A/13.6 | A/1.0 | A/18.2 |
| 17 | 17.3/A | 0.2/A | 14.8/A | 11.3/8.1 | 0.7/4.7 | 14.3/13.1 |

A, absent; CMAP, compound muscle action potential; NCV, nerve conduction velocity; TL, terminal latency.

fraction. Bland–Altman analysis result for the interobserver agreements and test–retest reproducibility are displayed in Table S1.

In the upper thigh muscles, significantly higher mean fat fractions were demonstrated in CMT patients compared with volunteers in all the measured muscle besides the adductor magnus (Table 5). In the lower thigh muscle, significantly higher mean fat fractions were seen in CMT patients in all the measured muscles. There was no significant difference in the mean muscle cross-sectional area between the two groups (Table 6). Wilcoxon signed rank test result for comparison between upper and lower thigh muscle fat fractions in the CMT patients showed significantly higher fat percentage in the vastus lateralis muscle of the lower thigh with no significant difference in other muscles (rectus femoris, vastus medialis, and semitendinosus) (Table S2).

The agreement between the two radiologists for semiquantitative analysis was almost perfect (kappa value of 0.843). There was disagreement of grading in nine muscles (9/408, 2.20%; Grade 0 vs. 1, two cases; Grade 1 vs. 2, six cases; and Grade 0 vs. 2, one case), all of which belonged to the patient group. One of the readers' data was used for analysis. All the upper thigh muscles were Grade 0 in volunteers (100%, 204/204). The results in CMT patients showed majority of muscles rated as Grade 0 (86.3%, 176/204), followed by Grade 1 (12.7%, 26/204), and Grades 2 and 4

**Table 4.** Interobserver agreement and test–retest reproducibility of muscle fat quantification

| | | Interobserver agreement | | | | Test–retest reproducibility (R1/R2) | | | |
|---|---|---|---|---|---|---|---|---|---|
| | | Upper thigh | | Lower thigh | | Upper thigh | | Lower thigh | |
| | | ICC | 95% CI | ICC | 95% CI | ICC | 95% CI | ICC | 95% CI |
| Rectus femoris | Right | 0.91 | 0.84–0.96 | 0.89 | 0.79–0.94 | 0.96/0.97 | 0.91–0.98/0.94–0.99 | 0.95/0.97 | 0.90–0.97/0.95–0.99 |
| | Left | 0.95 | 0.90–0.97 | 0.83 | 0.70–0.91 | 0.95/0.97 | 0.90–0.97/0.94–0.99 | 0.99/0.98 | 0.98–1.00/0.96–0.99 |
| Vastus lateralis | Right | 0.90 | 0.82–0.95 | 0.99 | 0.99–1.00 | 0.91/0.94 | 0.83–0.95/0.89–0.97 | 1.00/1.00 | 1.00–1.00/1.00–1.00 |
| | Left | 0.86 | 0.75–0.93 | 1.00 | 0.99–1.00 | 0.93/0.94 | 0.86–0.96/0.89–0.97 | 1.00/1.00 | 1.00–1.00/1.00–1.00 |
| Vastus medialis | Right | 0.95 | 0.91–0.98 | 0.97 | 0.95–0.99 | 0.87/0.95 | 0.76–0.93/0.90–0.97 | 0.99/0.99 | 0.99–1.00/0.99–1.00 |
| | Left | 0.98 | 0.95–0.99 | 0.96 | 0.93–0.98 | 0.95/0.94 | 0.90–0.97/0.89–0.97 | 0.99/0.99 | 0.99–1.00/0.98–1.00 |
| Semitendinosus | Right | 0.99 | 0.98–1.00 | 1.00 | 1.00–1.00 | 1.00/1.00 | 1.00–1.00/1.00–1.00 | 1.00/1.00 | 1.00–1.00/0.99–1.00 |
| | Left | 0.94 | 0.89–0.97 | 1.00 | 0.99–1.00 | 0.89/1.00 | 0.79–0.94/0.99–1.00 | 1.00/1.00 | 1.00–1.00/1.00–1.00 |
| Biceps femoris | Right | NA | NA | 1.00 | 1.00–1.00 | NA | NA | 1.00/1.00 | 1.00–1.00/1.00–1.00 |
| | Left | NA | NA | 0.98 | 0.97–0.99 | NA | NA | 1.00/1.00 | 0.99–1.00/1.00–1.00 |
| Adductor magnus | Right | 0.83 | 0.70–0.91 | NA | NA | 0.94/0.96 | 0.89–0.97/0.92–0.98 | NA | NA |
| | Left | 0.91 | 0.84–0.95 | NA | NA | 0.67/0.99 | 0.47–0.83/0.99–0.99 | NA | NA |
| Gracilis | Right | 0.91 | 0.83–0.95 | 0.98 | 0.95–0.99 | 0.98/0.99 | 0.97–0.99/0.98–0.99 | 1.00/1.00 | 0.99–1.00/0.99–1.00 |
| | Left | 0.91 | 0.84–0.96 | 0.97 | 0.93–0.98 | 0.99/0.99 | 0.99–1.00/0.98–1.00 | 0.99/0.99 | 0.99–1.00/0.99–1.00 |

CI, confidence interval; ICC, intraclass coefficient; NA, not applicable; R1, Reviewer 1; R2, Reviewer 2.

**Table 5.** Comparison of thigh muscle fat quantification between healthy volunteers and CMT patients

| | Rectus femoris | Vastus lateralis | Vastus medialis | Semitendinosus | Adductor magnus | Biceps femoris | Gracilis |
|---|---|---|---|---|---|---|---|
| Upper thigh | | | | | | | |
| Volunteers | 3.066 ± 1.313 | 3.587 ± 1.425 | 3.730 ± 1.513 | 5.238 ± 2.181 | 3.195 ± 1.202 | N/A | 5.349 ± 1.914 |
| CMT patients | 4.916 ± 2.939 | 4.649 ± 1.854 | 5.669 ± 2.818 | 11.473 ± 11.965 | 4.581 ± 3.581 | N/A | 10.849 ± 5.754 |
| *P* value | <0.001* | 0.011* | 0.001* | <0.001* | 0.109 | N/A | <0.001* |
| Lower thigh | | | | | | | |
| Volunteers | 2.684 ± 1.068 | 4.298 ± 1.585 | 3.273 ± 1.547 | 5.199 ± 1.691 | N/A | 4.231 ± 2.691 | 6.185 ± 2.760 |
| CMT patients | 6.694 ± 6.277 | 9.248 ± 8.393 | 5.648 ± 3.565 | 11.410 ± 8.440 | N/A | 13.381 ± 16.369 | 14.062 ± 10.012 |
| *P* value | <0.001* | 0.003* | <0.001* | <0.001* | N/A | <0.001* | <0.001* |

Data are displayed as mean values (%) ± standard deviation. CMT, Charcot–Marie–Tooth disease; N/A, not applicable.
*Indicates statistical significance.

**Table 6.** Comparison of thigh muscle cross-sectional area between healthy volunteers and CMT patients

| | Rectus femoris | Vastus lateralis | Vastus medialis | Semitendinosus | Adductor magnus | Biceps femoris | Gracilis |
|---|---|---|---|---|---|---|---|
| Upper thigh | | | | | | | |
| Volunteers | 916.014 ± 222.276 | 1704.049 ± 356.582 | 693.467 ± 115.891 | 379.169 ± 97.406 | 2041.183 ± 493.057 | N/A | 278.711 ± 64.237 |
| CMT patients | 918.407 ± 252.904 | 1732.060 ± 334.948 | 732.520 ± 124.404 | 418.864 ± 120.585 | 2102.977 ± 365.292 | N/A | 273.254 ± 65.575 |
| *P* value | 0.973 | 0.658 | 0.433 | 0.357 | 0.193 | N/A | 0.946 |
| Lower thigh | | | | | | | |
| Volunteers | 263.305 ± 178.248 | 1617.485 ± 506.403 | 1432.448 ± 342.284 | 462.466 ± 122.657 | N/A | 1007.295 ± 249.165 | 220.881 ± 90.093 |
| CMT patients | 199.123 ± 112.889 | 1575.501 ± 535.228 | 1512.382 ± 180.755 | 448.270 ± 111.431 | N/A | 920.659 ± 276.730 | 231.924 ± 75.237 |
| *P* value | 0.496 | 0.734 | 0.170 | 0.734 | N/A | 0.586 | 0.563 |

Data are displayed as mean values ($mm^2$) ± standard deviation. CMT, Charcot–Marie–Tooth disease; N/A, not applicable.

(0.05%, 1/204). Fat fractions of each grade were as follows: Grade 0 (mean: 4.72; standard deviation, 2.61; range, 0.87–18.60), Grade 1 (mean: 14.40; standard deviation, 5.19; range, 7.07–26.34), Grade 2 (27.37%), and Grade 4 (72.08%) (Figure 4). Goutallier Grade 0 muscles in the CMT patient group (median ± standard deviation, 4.54 ± 3.03; interquartile range, 3.58–6.82) showed significantly higher mean fat fraction compared with that of the volunteer group (median ± standard deviation, 3.58 ± 1.86; interquartile range, 2.70–5.00) ($P < 0.001$).

There was a correlation between intramuscular fat fraction of the upper thigh vastus medialis and CMTNS with correlation coefficient of 0.5191 ($P < 0.05$) (Table S3). There was no correlation between fat fraction of other muscles and other clinical parameters. No significant correlation was found between BMI and thigh muscle fat fraction in either CMT patient or volunteer group (Table S4).

## Discussion

In this study, the intramuscular fat fraction of the thigh obtained using 3D multiple gradient echo Dixon-based MRI showed significantly higher mean values in the CMT patients compared to those in the volunteers for all the muscles besides the adductor magnus. The excellent results of interobserver agreement and test–retest reproducibility suggest that fat measurement using this technique is highly reliable. To our knowledge, little has been reported on MRI evaluation of fat infiltration of thigh muscles in CMT patients. The significant difference in the degree of intramuscular fat fraction in the thigh between the two groups demonstrated in our study may be attributed to the sensitivity of the 3D multiple gradient echo Dixon-based MRI technique, which may not have been revealed by less advanced MRI techniques. However, further study with larger number of enrolled subjects and longitudinal data is warranted to elucidate the true significance.

With the characteristic predominant distal muscle wasting in CMT patients, only a small proportion of patients are reported to develop severe thigh muscle weakness late in the clinical course.[1,23] Most studies in the past also focused on evaluation of fat infiltration in lower leg muscles.[11,12] A recent study by Morrow *et al*.[24] comparing the intramuscular fat fraction using a Dixon-based MRI technique between a CMT Type IA group and a volunteer group showed a significantly higher muscle fat fraction in the lower leg but not at the thigh level. Besides the clinical factors of the enrolled subjects, the difference between our study result and this recent study may be related to technical factors. A three-point Dixon technique, with no information regarding T2* correction, was used for fat quantification in the study of Morrow *et al*. while T2*-corrected six-point Dixon technique was used in our

**Figure 4** Boxplots showing distribution of fat fraction in 408 thigh muscles of all subjects in each Goutallier grade (A) and Goutallier Grade 0 muscles of volunteer and Charcot–Marie–Tooth disease patient group (B). Numbers in the parentheses represent number of the measured muscles. ○, outliers.

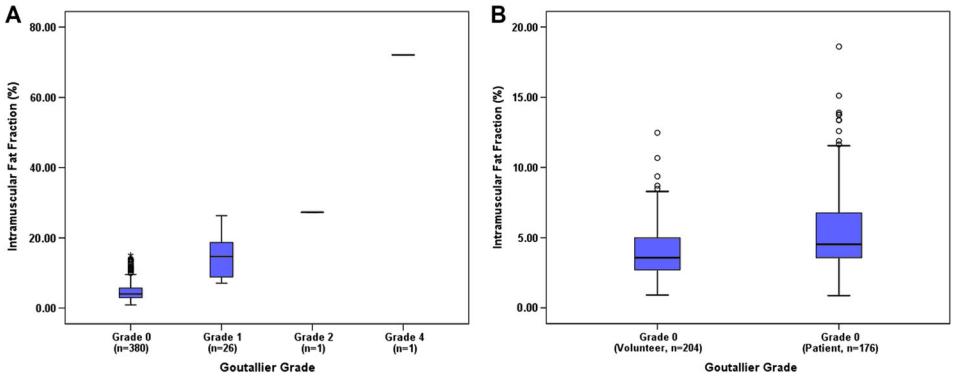


study. A previous study using MR spectroscopy as a reference standard reported that intramuscular fat quantification using T2*-corrected six-echo Dixon sequences showed a significantly better concordance with the spectroscopic data compared with those of T2*-corrected three-echo Dixon or non-T2*-corrected two-echo Dixon technique.[25] The importance of T2* correction has been proposed considering the presence of iron that causes local magnetic inhomogeneity and has been emphasized in liver fat quantification.[26] Skeletal muscles are also reported to contain non-negligible amounts of iron.[27] Also, it has been suggested that it is necessary to acquire at least six echoes for the optimal separation of water and fat signals with T2*-correction[28] as in our study. Our study result may suggest that 3D multiple gradient echo Dixon-based MRI can reveal intramuscular fat infiltration in the thigh which may be present at a relatively early stage of CMT. As with previous studies using Dixon-based MRI for evaluation of CMT or other neuromuscular disorder patients,[24,29,30] our result supports further application of this imaging technique for quantitative data acquisition regarding intramuscular fat fraction in future research.

Interobserver agreement and test–retest reproducibility were excellent for 3D multiple gradient echo Dixon-based MRI. Intramuscular fat quantification using Dixon-based quantitative MRI sequence is reported to show high interobserver and test–retest reproducibility.[16] Our study result is also in agreement with the previous results and suggests that Dixon-based MRI can provide a reliable fat measurement that is advantageous over subjective analysis based on Goutallier classification, which is reported to be highly observer dependent.[14,15] Goutallier Grade 0 muscles in the CMT patient group showed a significantly higher mean intramuscular fat fraction compared to that of the volunteer group (Figure 4). This result may imply that intramuscular fat measurement using a Dixon-based quantitative MRI sequence can be a more sensitive and objective tool for screening of muscular degeneration. In addition, 3D multiple gradient echo Dixon-based MRI could be obtained in a reasonable scan time (72.5 s) which was even shorter than the time taken for other conventional sequences (Table 1). Thus, it may easily be incorporated as part of a routine imaging sequence in neuromuscular disease patient evaluation.

None of the patients presented with subjective weakness of the thigh muscles, and only one patient showed slightly decreased strength for knee extension on physical examination. In this regard, our patients are subclinical in terms of proximal lower limb weakness, and intramuscular fat infiltration observed through 3D multiple gradient echo Dixon-based MRI may reflect early manifestation of the degeneration prior to clinically evident muscle weakness. Morrow *et al*. reported that calf muscle fat fraction measured using Dixon-based MRI significantly increased over 12 months in their cohort of CMT patients.[29] It would be beneficial to investigate the longitudinal change of thigh muscle fat fraction in a large cohort of CMT patients in the future. Furthermore, because substantial portion of the patients eventually develop hip muscle weakness,[31] it would be interesting to expand the evaluation to encompass hip muscles in future research.

In our study, a correlation was found between fat fraction of the upper thigh vastus medialis and CMTNS with correlation coefficient of 0.5191. A recent study by Morrow *et al.*[29] reported a strong correlation between calf muscle fat fraction with CMTNS. For thigh muscle, little is known about relation between the degree of fat infiltration and clinical status in CMT patients. Because our study mostly included patients with relatively early thigh muscle fatty degeneration, relation between thigh muscle fat fraction and clinical parameters should also be sought in patients with more advanced fat infiltration. Further investigation with larger cohort is needed.

Among a total 72 sets of 3D multiple gradient echo Dixon-based MRI, five image sets (6.9%) showed fat-water swap. Fat-water swaps are commonly encountered problems in Dixon technique attributed to phase shift errors.[32] To overcome this artefact by dealing with B0 field inhomogeneity, multipoint Dixon techniques have been developed.[32]


DOI: 10.1002/jcsm.12415

However, fat-water swaps still remain a problem in 3D multiple gradient echo Dixon-based MRI.[33] For further clinical application and exact measurement of intramuscular fat quantification by Dixon-based MRI, technical advances are warranted to overcome this issue.

There were several limitations in our study. First, the number of enrolled subjects was relatively small. However, we used an age- and sex-matched volunteers for comparison. Second, we lack longitudinal data of the thigh muscle fat fraction to clarify how these fat infiltration will change and affect clinical status in the future. Third, there may have been measurement errors in analyses. Fourth, the study population was limited to subjects in their 20s and 30s to evaluate MRI in detection of muscular changes in early stage of CMT because the disease onset usually occurs in the first two decades of life. Lack of patients with severe thigh muscular fatty atrophy and overt clinical symptom limited correlation of muscle fat fraction with clinical parameters such as muscle strength or electrophysiologic parameters of the sciatic nerve. Furthermore, the ability of fat quantification MRI for the distinction between intramuscular fat infiltration due to a normal age-related process and that in denervated muscle could not be sought. This may be beyond the range of our study.

In conclusion, muscle fat quantification using 3D multiple gradient echo Dixon-based MRI revealed a significant difference in the fat fraction in thigh muscle between CMT patients and normal volunteers, where intramuscular fat infiltration is less prominent compared with that in the calf muscle in CMT. A significant difference in fat fraction in Goutallier Grade 0 muscle between the two groups demonstrated in our result may suggest the sensitivity of the technique to indicate early fat infiltration which may be difficult to identify through visual assessment of T1-weighted image. This technique was highly reproducible and could be obtained in a relatively short scan time. Incorporation of 3D multiple gradient echo Dixon-based MRI as a part of the routine MRI for assessment of CMT and other neuromuscular disease patients may have clinical value.

## Online supplementary material

Additional supporting information may be found online in the Supporting Information section at the end of the article.

**Table S1.** Bland-Altman analysis for interobserver agreement and test-retest reliability
**Table S2.** Wilcoxon signed rank test for comparison of upper and lower thigh muscle fat fraction in the CMT patients
**Table S3.** Spearman's correlation analysis for the relation between thigh muscle fat fraction and clinical data
**Table S4.** Spearman's correlation analysis for the relation between body mass index and thigh muscle fat fraction

## Conflict of Interest

All of the authors (H.S.K, Y.C.Y, B.C, W.J, and J.G.C) declare that they have no conflict of interest.

## Acknowledgements

All of the authors certify that they comply with the ethical guidelines for publishing in the Journal of Cachexia, Sarcopenia and Muscle: update 2017.[34]

## References

1. Pareyson D, Marchesi C. Diagnosis, natural history, and management of Charcot–Marie–Tooth disease. *Lancet Neurol* 2009;**8**:654–667.
2. Garcia CA, Malamut RE, England JD, Parry GS, Liu P, Lupski JR. Clinical variability in two pairs of identical twins with the Charcot–Marie–Tooth disease type 1A duplication. *Neurology* 1995;**45**:2090–2093.
3. d'Ydewalle C, Krishnan J, Chiheb DM, Van Damme P, Irobi J, Kozikowski AP, et al. HDAC6 inhibitors reverse axonal loss in a mouse model of mutant HSPB1-induced Charcot–Marie–Tooth disease. *Nat Med* 2011;**17**:968–974.
4. Patzko A, Bai Y, Saporta MA, Katona I, Wu X, Vizzuso D, et al. Curcumin derivatives promote Schwann cell differentiation and improve neuropathy in R98C CMT1B mice. *Brain* 2012;**135**:3551–3566.
5. Sereda MW, Meyer zu Horste G, Suter U, Uzma N, Nave KA. Therapeutic administration of progesterone antagonist in a model of Charcot–Marie–Tooth disease (CMT-1A). *Nat Med* 2003;**9**:1533–1537.
6. Attarian S, Vallat JM, Magy L, Funalot B, Gonnaud PM, Lacour A, et al. An exploratory randomised double-blind and placebo-controlled phase 2 study of a combination of baclofen, naltrexone and sorbitol (PXT3003) in patients with Charcot–Marie–Tooth disease type 1A. *Orphanet J Rare Dis* 2014;**9**:199.
7. Rossor AM, Polke JM, Houlden H, Reilly MM. Clinical implications of genetic advances in Charcot–Marie–Tooth disease. *Nat Rev Neurol* 2013;**9**:562–571.
8. Murphy SM, Herrmann DN, McDermott MP, Scherer SS, Shy ME, Reilly MM, et al. Reliability of the CMT neuropathy score (second version) in Charcot–Marie–Tooth disease. *J Peripher Nerv Syst* 2011;**16**:191–198.
9. Haberlova J, Seeman P. Utility of Charcot–Marie–Tooth neuropathy score in children with type 1A disease. *Pediatr Neurol* 2010;**43**:407–410.
10. Gallardo E, Garcia A, Combarros O, Berciano J. Charcot–Marie–Tooth disease type 1A duplication: spectrum of clinical and magnetic resonance imaging features in leg and foot muscles. *Brain* 2006;**129**:426–437.
11. Gaeta M, Mileto A, Mazzeo A, Minutoli F, Di Leo R, Settineri N, et al. MRI findings, patterns of disease distribution, and muscle fat fraction calculation in five patients with Charcot–Marie–Tooth type 2 F disease. *Skeletal Radiol* 2012;**41**:515–524.

12. Chung KW, Suh BC, Shy ME, Cho SY, Yoo JH, Park SW, et al. Different clinical and magnetic resonance imaging features between Charcot–Marie–Tooth disease type 1A and 2A. *Neuromuscul Disord* 2008;**18**:610–618.
13. Slabaugh MA, Friel NA, Karas V, Romeo AA, Verma NN, Cole BJ. Interobserver and intraobserver reliability of the Goutallier classification using magnetic resonance imaging: proposal of a simplified classification system to increase reliability. *Am J Sports Med* 2012;**40**:1728–1734.
14. Shahabpour M, Kichouh M, Laridon E, Gielen JL, De Mey J. The effectiveness of diagnostic imaging methods for the assessment of soft tissue and articular disorders of the shoulder and elbow. *Eur J Radiol* 2008;**65**:194–200.
15. Alizai H, Nardo L, Karampinos DC, Joseph GB, Yap SP, Baum T, et al. Comparison of clinical semi-quantitative assessment of muscle fat infiltration with quantitative assessment using chemical shift-based water/fat separation in MR studies of the calf of post-menopausal women. *Eur Radiol* 2012;**22**:1592–1600.
16. Agten CA, Rosskopf AB, Gerber C, Pfirrmann CW. Quantification of early fatty infiltration of the rotator cuff muscles: comparison of multi-echo Dixon with single-voxel MR spectroscopy. *Eur Radiol* 2016;**26**:3719–3727.
17. Dixon WT. Simple proton spectroscopic imaging. *Radiology* 1984;**153**:189–194.
18. Karampinos DC, Yu H, Shimakawa A, Link TM, Majumdar S. T(1)-corrected fat quantification using chemical shift-based water/fat separation: application to skeletal muscle. *Magn Reson Med* 2011;**66**:1312–1326.
19. Goutallier D, Postel JM, Bernageau J, Lavau L, Voisin MC. Fatty muscle degeneration in cuff ruptures. Pre- and postoperative evaluation by CT scan. *Clin Orthop Relat Res* 1994;78–83.
20. Birouk N, Gouider R, Le Guern E, Gugenheim M, Tardieu S, Maisonobe T, et al. Charcot–Marie–Tooth disease type 1A with 17p11.2 duplication. Clinical and electrophysiological phenotype study and factors influencing disease severity in 119 cases. *Brain* 1997;**120**:813–823.
21. Shy ME, Blake J, Krajewski K, Fuerst DR, Laura M, Hahn AF, et al. Reliability and validity of the CMT neuropathy score as a measure of disability. *Neurology* 2005;**64**:1209–1214.
22. Compston A. Aids to the investigation of peripheral nerve injuries. Medical Research Council: Nerve Injuries Research Committee. His Majesty's Stationery Office: 1942; pp. 48 (iii) and 74 figures and 7 diagrams; with aids to the examination of the peripheral nervous system. By Michael O'Brien for the Guarantors of Brain. Saunders Elsevier: 2010; pp. [8] 64 and 94 Figures. *Brain* 2010;**133**:2838–2844.
23. Berciano J, Gallardo E, Garcia A, Infante J, Mateo I, Combarros O. Charcot–Marie–Tooth disease type 1A duplication with severe paresis of the proximal lower limb muscles: a long-term follow-up study. *J Neurol Neurosurg Psychiatry* 2006;**77**:1169–1176.
24. Morrow JM, Sinclair CD, Fischmann A, Machado PM, Reilly MM, Yousry TA, et al. MRI biomarker assessment of neuromuscular disease progression: a prospective observational cohort study. *Lancet Neurol* 2016;**15**:65–77.
25. Yoo YH, Kim HS, Lee YH, Yoon CS, Paek MY, Yoo H, et al. Comparison of multi-echo Dixon methods with volume interpolated breath-hold gradient echo magnetic resonance imaging in fat-signal fraction quantification of paravertebral muscle. *Korean J Radiol* 2015;**16**:1086–1095.
26. Westphalen AC, Qayyum A, Yeh BM, Merriman RB, Lee JA, Lamba A, et al. Liver fat: effect of hepatic iron deposition on evaluation with opposed-phase MR imaging. *Radiology* 2007;**242**:450–455.
27. Beard JL. Iron biology in immune function, muscle metabolism and neuronal functioning. *J Nutr* 2001;**131**:568S–579S, discussion 580S.
28. Reeder SB, Robson PM, Yu H, Shimakawa A, Hines CD, McKenzie CA, et al. Quantification of hepatic steatosis with MRI: the effects of accurate fat spectral modeling. *J Magn Reson Imaging* 2009;**29**:1332–1339.
29. Morrow JM, Evans MRB, Grider T, Sinclair CDJ, Thedens D, Shah S, et al. Validation of MRC Centre MRI calf muscle fat fraction protocol as an outcome measure in CMT1A. *Neurology* 2018;**91**:e1125–e1129.
30. Willis TA, Hollingsworth KG, Coombs A, Sveen ML, Andersen S, Stojkovic T, et al. Quantitative muscle MRI as an assessment tool for monitoring disease progression in LGMD2I: a multicentre longitudinal study. *PLoS ONE* 2013;**8**:e70993.
31. Verhamme C, van Schaik IN, Koelman JH, de Haan RJ, Vermeulen M, de Visser M. Clinical disease severity and axonal dysfunction in hereditary motor and sensory neuropathy IA. *J Neurol* 2004;**251**:1491–1497.
32. Guerini H, Omoumi P, Guichoux F, Vuillemin V, Morvan G, Zins M, et al. Fat suppression with Dixon techniques in musculoskeletal magnetic resonance imaging: a pictorial review. *Semin Musculoskelet Radiol* 2015;**19**:335–347.
33. Henninger B, Zoller H, Kannengiesser S, Zhong X, Jaschke W, Kremser C. 3D multiecho Dixon for the evaluation of hepatic iron and fat in a clinical setting. *J Magn Reson Imaging* 2017;**46**:793–800.
34. von Haehling S, Morley JE, Coats AJS, Anker SD. Ethical guidelines for publishing in the journal of cachexia, sarcopenia and muscle: update 2017. *J Cachexia Sarcopenia Muscle* 2017;**8**:1081–1083.